Yunjie Xu[1]

School of Technology, Zhejiang Agricultural & Forestry University, Lin'an, China(1)

Research on Hybrid Ray-tracing at 2.4 GHz in Man-Made Forests

Abstract. *Since the environment in the forest is relatively complicated and there's a necessity to avoid the dead zone of signal diffraction when laying wireless sensor in the forest, the integration of SBR and UTD is applied to study the impact of 2.4GHz radio-frequency signal on the path loss characteristics in the forest. This paper achieved the ray location from the receive pint to field point by using back-ray tracing method and computed the response electric field relative to each ray by using UTD. Take the poplar planted forest for instance. The measured value and simulated value were compared, finding good consistency between them, which indicates that SBR and UTD can effectively predict the path loss characteristics in the forest.*

Streszczenie. *W artykule przedstawiono zagadnienie rozprowadzania pola sieci bezprzewodowej w obszarze leśnym. Zastosowane rozwiązania (SBR, UTD) pozwoliły na skuteczną lokalizację i przesył informacji przy zastosowaniu fal 2.4GHz. Wyniki symulacyjne porównano z wynikami pomiarów, przeprowadzonych w lesie topolowym. (**Badania hybrydowego systemu śledzenia fal promieniowania 2.4GHz w sztucznym lesie**).*

Keywords: man-made forests, Inverse Ray-tracing, standing tree, 2.4 GHz.
Słowa kluczowe: sztuczny las, śledzenie wsteczne promieni, drzewo stojące, 2,4GHz.

1. Introduction

When compared the 2GHz signal propagation problem with these applied ray tracing techniques, regardless their common points, we still identified the following main difference between them:

1. It is necessary to consider the impact of phase and polarization in UHF and the sources are coherent.

2. Geometrical optics almost gives no consideration to the wedge diffraction which, however, plays an important role in UHF as its existence enables the field to reach to the deep shadow zone that is impossible in geometrical optics.

3. Reflection in geometrical optics mainly focuses on diffusion while in UHF, it is the direct reflection that in domination. Of course, the difference between wireless transmission and visibility decreases with the increase of frequency [3].

Given the abovementioned differences, it is impossible to apply the existing visible ray tracing techniques to solve the signal propagation in UHF directly. Therefore, it is necessary to carry out a detail study on the transmission mode of electromagnetic wave in the planted forest in order to achieve a thorough research on the transmission law of UHF in it [6, 14].

2. Signal scanning in the forest as well as its visibility judgment

Ray tracing requires detail site information of specific environment. The transmission mechanisms of electromagnetic wave in space are mainly collineation, reflection, diffraction and transmission [2]. As far as the absorbing screen environment of UHF is concerned, as the tree trunk is non-transparent, we can only give consideration to the following four situations: collineation, locality principle-consistent reflection, diffraction as well as the combination of reflection and diffraction, neglecting the impact of transmission [1]. UHF electromagnetic wave propagation in the absorbing screen shows obvious damping, making it possible to neglect secondary or multiple reflection, diffraction as well as their combination.

2.1. Horizontal scanning

According to the characteristic of signal wave polarization in the forest, we first apply the horizontal scanning algorithm here and give no consideration to the tree height for temporary [4]. Before the horizontal search, the table of visible wedge including emission source point, receiving field point, all wedge diffraction points, etc. shall be established and all possible paths from receiving field point to emission source point shall be determined, which will be combined with the information storage of stumpage model to accomplish the ray horizontal scanning [5, 9]. The source point in information storage of the stumpage model equals to the origin of coordinates of the rectangular coordinate system, field point equals to the receiving point, and diffraction point equals to the intersection point of edges and scanning line [10, 15]. The visible surface of source point and field point shall be determined in advance since we have to consider once and secondary diffraction as well as once and secondary reflection.

1) Once diffraction scanning

Take the stumpage arrangement method of row 3 and line 3 for example. As shown in Fig.1, from which we can see that the base point Sp and receiving point Rx can only be reached through diffraction. First, determine the scanning base point Sp and then draw out the tangential line of all visible columnar, obtaining 13 scanning contact points shown in Fig.2. Those cross the contact points belong to the vertical curves of the columnar, or known as vertical wedge. Simplify the stumpage based on the initial edge whose prism is the tangential line. Finally, examine and compute all scanning lines within the scanning zone according to certain order. The connecting line between base point Sp and contact point is the scanning line. Divide the space into two zones according to the situation of scanning line and cylindrical surface tangency: visible zone and invisible zone. Viewed from Fig.2a), the 13 scanning contact points divided the space into three visible zones and 2 invisible zones. List the three visible zones obtained through once diffraction, shown in table1.

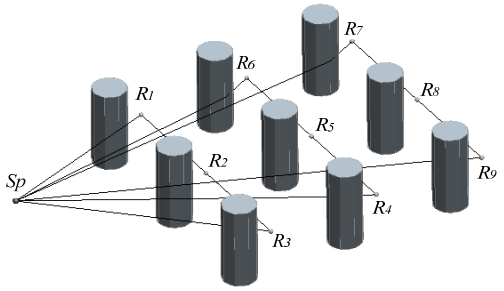

Fig.1.The standing tree 3D modelling map of once horizontal scanning

2) Secondary diffraction scanning

After the visible surface table of once diffraction scanning of the source point and field point was obtained, it is required to calculate the secondary diffraction scanning

line of some scanning lines, that is, to obtain the visible surface table of secondary diffraction points [7, 11]. Point 4 is the diffraction point determined by once diffraction and from Fig.2b), we can see that 4_1, 4_2, 4_3, 4_4 and 4_5 are five scanning contact points of secondary diffraction, which divided the space into two visible zones and three invisible zones. The visible zones of secondary diffraction can be obtained through Fig.3, shown in table2.

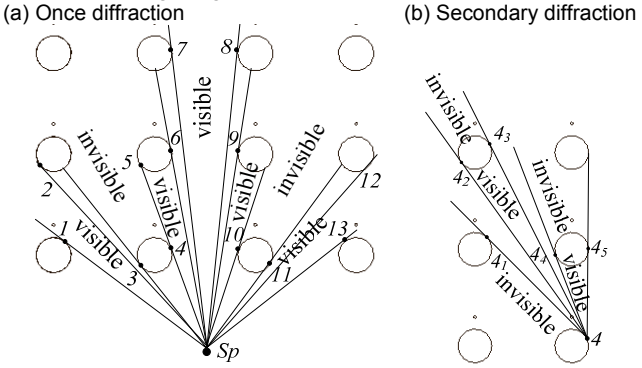

Fig.2.The visible zones of once diffraction

Table. 1. The visible zones table of once diffraction

Source point	Visible zones1	Visible zones 2	Visible zones3
1	Sp-1-2-3	Sp-4-5-6-7-8-9-10	Sp-1_1-1_2-1_3

Table. 2. The visible zones table of secondary diffraction

Source point	Visible zones 1	Visible zones 2	Visible zones 3
4	4-4_1-4_2-4_3-4_4	4-4_2-4_3	Sp-1_1-1_2-1_3

2. 2.Vertical scanning

In practical application, the radio wave propagation environment is spatial, and the location of emission source point and receiving field point as well as tree height will exert impact on the visible surface table. Therefore, it is necessary for us to introduce vertical scanning based on the horizontal scanning to adapt to the forest environment. According to the literatures, the forest crown is attenuation screen and the radio wave propagation through the upper forest mainly focuses on lateral wave, thus making the vertical scanning only effective to the sensor located in the specific position before the tree [8, 12, 13]. Therefore, we can only identify the diffraction across the tree top part. Just if the sensor was placed back of the tree, it can only find invisible zones. The signal propagation is calculated according to the signal propagation in attenuation screen and free space.

3. Solution of Diffraction Path in Back Algorithm

3.1. Solution of once diffraction path

The simplified model of once diffraction space of standing trees is shown in Fig.3. Simplified model of once diffraction space. Where Sp is source point , Rx is receiver point , Q is diffraction point.

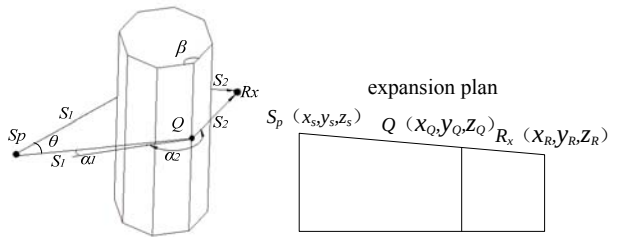

Fig.3.The simplified model of once diffraction

There are two methods can be used to solve the diffraction points. The first one is the specific solution when the receiving point Rx is known, and the second is the diffraction point solution of no specific direction when both the diffraction pint and receiving point are unknown.

The procedure of the first method is as follows:

1) Establish the visible zone table of once diffraction and determine the common visible wedge of emission point and field point;

2) After finish the layout of emission point and sensor nodes, the coordinates of source point and field point can be known. Choose one common visible wedge and calculate the diffraction point value through the equation set 1.

3) Develop the incidence face and diffraction face in one flat surface along the vertical surface line of column which locates in the diffraction point Q, results shown in Figure 3.1. Calculate the coordinate of diffraction point z in right-angled trapezoid, and $Z_Q = Z_R + |Z| \cdot$

$$|Z| = \frac{\sqrt{(x_Q - x_R)^2 + (y_Q - y_R)^2}}{\sqrt{(x_Q - x_R)^2 + (y_Q - y_R)^2} + \sqrt{(x_S - x_Q)^2 + (y_S - y_Q)^2}} (z_S - z_R) \quad (1)$$

4) Effectiveness judgment. After the diffraction point is obtained, it needs to determine whether the diffraction point lies in the finite-length vertical wedge. If zQ≤H1, the diffraction path exists; otherwise, no diffraction path exists.

5) Repeat the above steps and choose the common visible vertical wedges of other living woods until all the common visible wedges are calculated.

Fig.4 is the vector ray tracing map of any point Q in right-angle wedge by using the second solution, where $\overrightarrow{S_p}$ is the radius vector of the emission point that is ds away from the right-angle wedge edge, Q is the radius vector of diffraction point that is rd away from the emission point, $\vec{O}$ is the radius vector of observation point that locates on the circle which takes one point of wedge edge as its center, d0 as its radius and rs away from the diffraction point, and $\overrightarrow{p_1}$ and $\overrightarrow{p_2}$ are the radius vectors of two endpoints of the finite-length right-angle wedge.

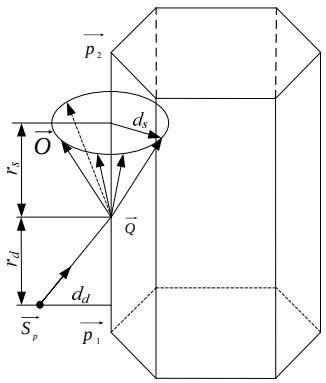

Fig.4.The vector ray tracing map of any point in wedge

The radius vector of diffraction point on the wedge is:

$$\vec{Q}(t) = \overrightarrow{p_1} + t(\overrightarrow{p_2} - \overrightarrow{p_1}) \quad (2)$$

The four vector distances ds、da、rd、rs can be expressed as follows:

$$d_d = \sqrt{(\overrightarrow{S_p} - \overrightarrow{p_1}) \cdot (\overrightarrow{S_p} - \overrightarrow{p_1}) - \left[(\overrightarrow{p_2} - \overrightarrow{p_1}) \cdot (\overrightarrow{S_p} - \overrightarrow{p_1}) / \left|\overrightarrow{p_2} - \overrightarrow{p_1}\right|\right]^2} \quad (3)$$

$$d_s = \sqrt{(\vec{O} - \overrightarrow{p_1}) \cdot (\vec{O} - \overrightarrow{p_1}) - \left[(\overrightarrow{p_2} - \overrightarrow{p_1}) \cdot (\vec{O} - \overrightarrow{p_1}) / \left|\overrightarrow{p_2} - \overrightarrow{p_1}\right|\right]^2} \quad (4)$$

$$r_d(t) = (\vec{Q}(t) - \overrightarrow{S_p}) \cdot (\overrightarrow{p_2} - \overrightarrow{p_1}) / \left|\overrightarrow{p_2} - \overrightarrow{p_1}\right| \quad (5)$$

(6) $$r_s(t) = (\vec{Q} - \vec{Q}(t)) \cdot (\vec{p_2} - \vec{p_1}) / \left| \vec{p_2} - \vec{p_1} \right|$$

Keller pointed out that the included angle between edge diffraction ray and wedge edge equals to the included angle between incidence ray and wedge edge.

(7) $$\frac{r_d}{d_d} = \frac{r_s}{d_s}$$

Substitute (2),(3),(4),(5),(6) into (7), and get the parameter t after simplification:

(8) $$t = \frac{(\vec{p_2} - \vec{p_1})}{\left| \vec{p_2} - \vec{p_1} \right|^2} \cdot \left[\frac{(\vec{S_p} d_s + \vec{O} d_d)}{d_s + d_d} - \vec{p_1} \right]$$

Make judgment on the parameter t. If $t \in (0,1)$, there exist one diffraction point. Substitute t into (2) and we can obtain the location of the diffraction point.

3.2. Solution of secondary diffraction path

Under the ultimate state (weakest receive signals), when the sensor is placed back of the tree with the shortest distance with the tree, there's only one situation that enables the ray to reach to the receiving point in shadow zone (back of the tree) in secondary diffraction. The path search method of secondary diffraction is similar to that of once diffraction, Will not repeat.

4. UTD field strength computation

According to the geometric theory of diffraction, we can get the geometric diagram of vertical wedge diffraction, shown in Fig.5.

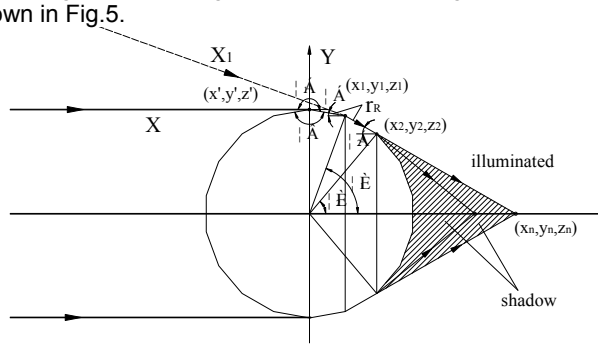

Fig.5. The simplified model of wedge diffraction

Without loss of generality, the receiver points are assumed to lie in the plane Z=0 because of the translation symmetry along Z (trunk height direction). With the foregoing assumptions, the diffracted field through the edge for standing tree is given as follows:

(9) $$E(x_1, y_1, 0) = A_0 \frac{jk}{4\pi} \int_0^{+\infty} \int_{-\infty}^{+\infty} (1 + \cos\alpha) \frac{e^{-jkr_R}}{r_R} d_{z'} d_{y'}$$

Where the distance from the integration point to the receiver point $r_R = \sqrt{x_1^2 + (y_1 - y)^2 + (z')^2}$.

To perform the z' integration in Eq. (9), the primary contribution to the integral comes from a region of z' that is given by the Fresnel zone, which is small compared with x, i.e., x>>λ. The center of this region is the stationary-phase point, where the derivative of the exponent krR with respect to z vanishes. rR in the denominator and cosα will hardly vary and can be treated as constants.

rR can be expanded to the second order according to ρR, with $\rho_R = \sqrt{x_1^2 + (y_1 - y')^2}$, and thus, $r_R = \rho_R + (z')^2 / 2\rho_R$.

Substituting rR into Eq. (9), the integration over z' is reduced as follows:

(10) $$E(x_1, y_1, 0) = A_0 \frac{jk}{4\pi} \int_0^{+\infty} \int_{-\infty}^{+\infty} (1 + \cos\alpha) \frac{e^{-jkr_R}}{r_R} d_{z'} d_{y'}$$

(11) $$E(x_1, y_1, 0) \approx A_0 \frac{jk}{4\pi} \int_0^{+\infty} (1 + \cos\alpha) \frac{e^{-jk\rho_R}}{\rho_R} \left[\int_{-\infty}^{+\infty} \exp\left[-jk \frac{(z')^2}{2\rho_R} \right] dz' \right] dy'$$

Using the substitution $u = z' e^{j\pi/4} \sqrt{k/2\rho_R}$ to perform integral transform, Eq. (10) changes into the following:

(12) $$E(x_1, y_1, 0) \approx A_0 \frac{jk}{4\pi} \int_0^{+\infty} (1 + \cos\alpha) \frac{e^{-jk\rho_R}}{\rho_R} e^{j\pi/4} \sqrt{\frac{2\pi\rho_R}{k}} dy'$$
$$= A_0 \frac{e^{j\pi/4}}{2} \sqrt{\frac{k}{2\pi}} \int_0^{+\infty} (1 + \cos\alpha) \frac{e^{-jk\rho_R}}{\sqrt{\rho_R}} dy'$$

Similarly, the expression $\rho_R = \sqrt{x_1^2 + (y_1 - y')^2}$ can be expanded to the second order as $\rho_R = \rho - y' \frac{y_1}{\rho}$ according to ρ, with $\rho = \sqrt{x_1^2 + y_1^2}$. θ1 is the angle between the x axis and the line from the edge to the receiver point, and thus, $\sin\theta_1 = y_1/\rho$.

Using the substitution $v = y' e^{-j\pi/4} \sqrt{k/\rho}$ to perform integral transform, Eq. (12) turns into the following:

(13) $$E(x_1, y_1, 0) = A_0 \frac{e^{j\pi/4}}{2} \sqrt{\frac{k}{2\pi}} \left[\int_0^{+\infty} (1 + \cos\alpha) \frac{e^{-jk\rho_R}}{\sqrt{\rho_R}} dy' \right]$$
$$\approx A_0 \frac{e^{j\pi/4}}{2} \sqrt{\frac{k}{2\pi}} (1 + \cos\theta) \frac{e^{-jk\rho}}{\sqrt{\rho}} \int_0^{+\infty} \exp\left(jky' \frac{y}{\rho} \right) dy'$$
$$= A_0 e^{-jk\rho} \bullet \left(-\frac{e^{j\pi/4}}{\sqrt{2\pi k\rho}} \frac{1 + \cos\theta}{2\sin\theta} \right)$$

When performing the integration in Eq. (13), k is given a vanishingly small negative imaginary part, as appropriate for atmospheric absorption, to ensure convergence at the lower limit. However, after the integration, k can be taken to be real. When the diffraction coefficient $D(\theta_1) = -e^{j\pi/4}(1+\cos\theta)/(2\sin\theta\sqrt{2\pi k\rho})$, and when Einc=A0e-jkx is substituted into Eq. (13), the following is derived [17]:

(14) $$E(x_1, y_1, 0) = A_0 e^{-jk\rho} D(\theta_1) = E^{\text{inc}}(0, y', z') e^{-jk\rho} D(\theta_1)$$

In the radio wave propagation environment in the forest, all simplified diffraction wedges are medium wedges of limited conductivity, which requires to calculating its diffraction coefficient $\overline{D}$.

(15) $$\overline{D} = D^{(1)} + R_0 R_n D^{(2)} + R_0 D^{(3)} + R_n D^{(4)}$$

Where $D^{(1)} = \frac{-\exp(-\frac{j\pi}{4})}{2n\sqrt{2\pi k}} \times \cot\gamma^{(i)} F(2kLn^2 \sin^2\gamma^{(i)})$

$$\gamma^{(1)} = [\pi - (\alpha_2 - \alpha_1)]/2n$$
$$\gamma^{(2)} = [\pi + (\alpha_2 - \alpha_1)]/2n$$
$$\gamma^{(3)} = [\pi - (\alpha_2 + \alpha_1)]/2n$$
$$\gamma^{(4)} = [\pi + (\alpha_2 + \alpha_1)]/2n$$

R_0 is the reflection coefficient of 0 face, R_n is the reflection coefficient of face, $n\pi - \alpha_2$ angle of incidence.

Where , F(x)is the transition functions, and is given by

$$F(x) = 2j\sqrt{x} \exp(jx) \int_{\sqrt{x}}^{\infty} \exp(-j\tau^2) d_\tau$$

L is the parameter of distance, and is given by

$$L = s \cdot \sin^2\left(\frac{\theta}{2} - \frac{2\pi}{n}\right)$$

The reflection coefficient R is expressed as:

$$R = R_\perp e_\perp^i e_\perp^r + R_\parallel e_\parallel^i e_\parallel^r$$

S_1 is incident wave process, S_3 is reflected wave process. $R_\perp$, $R_\parallel$ is Vertical polarization and parallel polarization

of the reflection coefficient. α_1 is angle of incidence, ε is the complex permittivity, $\varepsilon = \varepsilon_r - j60\sigma\lambda$ is the relative dielectric constant.

5. Study on the 2.4GHz path loss character-istics

First, study the contribution of ray to the strength of receiving signals. Choose the planted poplar forest as the main sampling tree. Just as shown in Fig.6, collineation and reflection play the dominate role in signal receiving in illumination zone while the diffraction signal plays the most critical role in transition zone.

Fig.2a) is the simulated zone and the area lies behind the shadow border is transition and invisible zone. Micaz integrated node module is applied for emission and field intensity indicator is applied for receiving. From Fig.7, we can see good consistency between the measured value and simulated value, which indicates that in 2.4GHz frequency, the ray tracing method is able to effectively predict the path loss characteristics in the planted forest environment. Furthermore, the predicted values of path loss on the test point are generally smaller that the measured values, which is caused by the simplification of planted forest environment and living woods during simulation as well as the error of propagation model. For example, the simulated value neglects the impact of secondary or multiple diffraction and reflection.

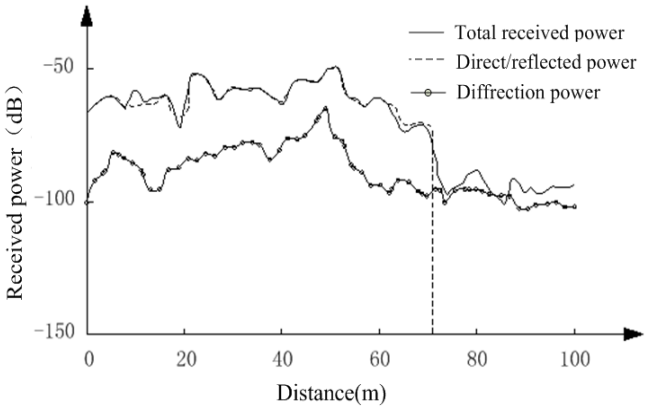

Fig.6.Contributions to the received signals

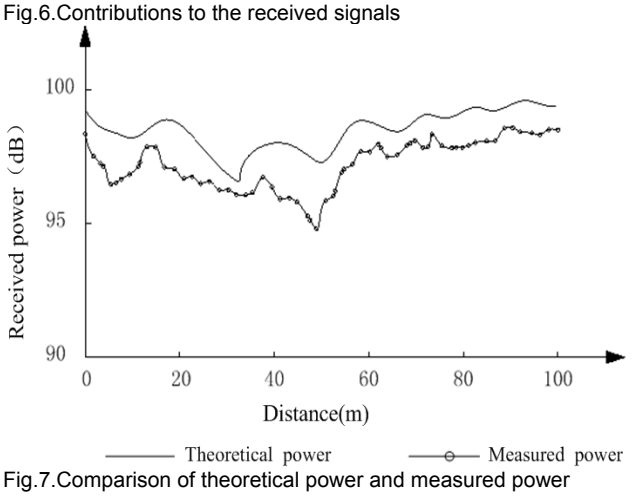

Fig.7.Comparison of theoretical power and measured power

6. Conclusion

In conclusion, the layout of sensors for the measurement of standing tree and the problem of Inverse Ray-tracing and the blind region of diffraction in optimization are discussed. The integration of SBR and UTD is applied to study the impact of 2.4GHz radio-frequency signal on the path loss characteristics in the forest. The feasibility and validity of computing the Inverse Ray-tracing of standing tree in plantation is verified using theoretical analysis and simulation. What's more, the key point of wireless network planning and design lies in the research about the impact of transmitting antenna's height and location on the path loss characteristics. Therefore, the theoretical research of this paper is of practical significance.

Acknowledgements

This work was supported in part by the National Natural Science Foundation of China (Grant No. 30972425) and the Natural Science Foundation of Zhejiang Province of China (Grant No. LY12C16003). Thanks for the help.

REFERENCES

[1] J.H.W hltteker, Frresnel-Kirchhoff theory applied to terrain diffraction problems, Radio Sci, 25(1990),837-851.

[2] Y.J. Xu, W.B. Li, Propagation path loss prediction model of multi-sensor network in forest. Procedia Engineering. 15 (2011),412-414.

[3] M.G. Wang, Geometrical Theory of Diffraction, China Xidian University Press, Beijing: 1989.

[4] X. Wen, Y.X. Xie, Diffraction over a Flat-Topped Terrain Obstacle with Bevel Edge, Chinese Journal of Electronics, 23(1995),81-83.

[5] Y.J. Xu, W.B. Li, Strength Prediction of Propagation loss in Forest Based on Genetic-SVM Classifier, 2010 Second International Conference on Future Computer and Communication, 03(2010), 251-254.

[6] Henry L. Bertoni, Radio propagation for modern wireless system, Publishing House of Electronics industry. Beijing: 2002.

[7] Zhang, YB, Bian, X, Liu, Y, Qu, HM. Agglomeration Mechanism of Horizontally Integrated Multinationals under D-S Model of Limited-Number Enterprises. Applied Mathematics & Information Sciences,05(2011) ,17-23.

[8] B.B. Baker and E.T. Copson. The Mathematical Theory of Huygens Principle,2nd ed., Qxford University Press,London(1953).

[9] Y. S. Meng.Path loss modeling for near-ground VHF radio-wave propagation through forests with tree-canopy reflection effect. Progress In Electromagnetics Research M, 12(2010),131-141.

[10] Sharma，Mahadev. Height-diameter equations for boreal tree species in Ontario using a mixed-effects modeling approach. Forest Ecology and Management,249(2007),No.03,187-198.

[11] S.S.Seker. VHF/UHF Radio Propagation Through Forests：Modeling and Experimental Observations，IEEE Proceedings-H, 139(1992),No.01,72-78.

[12] S.S.O. Burgess,M.L. Kranz, N.E. Turner. Harnessing wireless sensor technologies to advance forest ecology and agricultural research. Agricultural and Forest Meteorology,150(2010),No. 1,30-37.

[13] Musaloiu-E et al., Life Under Your Feet:A Wireless Soil Ecology Sensor Network,Proc. 3rd Workshop on Embedded Networked Sensors,2006.

[14] Pathak,P. H., Huang,J.An MM-GTD Analysis of the Radiation from Slots in Planar and Cylindrical Perfectly-Conducting Structures with a Surface Impedance Patch. Defense Technical Information Center OAI-PMH Repository (United States). Ohio state univ columbus electrosciencelab,2002.

[15] Nicolas No´e and Fran¸cois Gaudaire. Reflection on curved surfaces in a 2.5D ray-tracing method for electromagnetic waves exposure prediction in urban areas. General Assembly and Scientific Symposium,8(2011),13-20.

[16] Paul R. ROUSSEAU and Prabhakar PATHAK， A Time Domain Uniform Geometrical Theory of Slope diffraction for a Curved Wedge. Turk J Elec Engin,10(2002),No.2,385-398.

[17] Zeng Ming, Li Shulei, Liu Hongzhi, Xue Song, Li Lingyun, Demand Response Resource Value Post-Evaluation Model Based on Fuzzy-Rough Sets, Advanced Management Science, 1 (2011), No.1, 1-10

***Authors**: Yunjie Xu are with the School of Technology, Zhejiang Agricultural & Forestry University, Lin'an, China .*
(E-mail: xyj9000@163.com).